Indian Journal of Engineering & Materials Sciences
Vol. 27, December 2020, pp. 1112-1117

Synthesis of carbon nanotube fiber *via* direct spinning for conducting wires

Pallvi Dariyal[a,b], Abhishek Kumar Arya[a,b], Bhanu Pratap Singh[a,b]*, Sanjay Ranganth Dhakate[a,b]*

[a]CSIR-National Physical Laboratory, New Delhi 110 012, India

[b]Academy of Scientific and Innovative Research (AcSIR), Ghaziabad, Uttar Pradesh 201002, India

Received: 25 August 2020

The commercial conducting materials (Cu, Ag, Al etc.) have achieved their saturation due to their high density and Joule's heating effect in terms of efficiency. In this outlook, carbon nanotubes (CNTs) are the most versatile, light weight and high electrically conducting material for advance generation. But it is difficult to weave them for commercialization. For the growth of 3-D CNT assemblies such as CNT fiber, CNT sheet, CNT rope and CNT ribbon, direct spinning is the most suitable technique because of its simplicity for continuous growth of CNT fiber. In the present work, different growth parameters were analysed for the growth of CNT fibers. The growth of CNT fibres has been carried out through direct spinning of as-synthesised CNT aerogel. CNT fibers were grown successfully *via* optimizing different processing parameters like temperature, pressure and argon to hydrogen ratio. The morphology of as-spun fibers was investigated *via* microscopic techniques such as optical microscopy, SEM and TEM. Moreover, the defects and metallicity of as-spun fibers have been analysed using Raman spectroscopy. The change in resistance with change in temperature was also measured for quality of as-made CNT fiber which shows metallic behavior as CNT fiber has positive temperature coefficient. Above 151K, conducting CNTs are dominating and below this temperature, semiconducting CNTs are showing their nature in R v/s T curve. Furthermore, the measured electrical conductivity of as-made fiber is 3.9×10^3 S/m. These as-spun metallic fibers can outperform the currently used Cu wire. Hence, as-synthesized conductive CNT fibers have great potential as conducting wires.

Keywords: Joule's heating effect, CNT aerogel, 3D-CNT assemblies, Direct spinning, Temperature coefficient

1 Introduction

Keeping an eye on the growing field of electrical engineering, light weight and highly electrically conducting materials are desirable for future electronics and nano-electronic devices for nano-sensors, different energy storage applications, automobile industries and aircraft manufacturers. The commercial conducting materials have achieved their saturation in terms of efficiency due to high density and efficacy. The carefully engineered conducting nano-structures may increase the device efficiency and reduce its size. Hence advanced lightweight and reliable alternatives to traditional conducting materials are being researched and implemented. The carbon nano-structures are suitable alternative of conventional conducting materials due to their high electrical conductivity (derived from graphite structure) and low density. Among them, carbon nanotubes (CNTs) are the most versatile material for advanced generation due to high electrical conductivity[1], high flexibility and good environmental stability[2]. These nanotubes are long hollow conductors where delocalized electrons of sp^2 hybridized carbon are free to move along the axial direction[3]. Therefore, CNTs are also termed as ballistic conductors. Due to such fascinating electric properties such as high ampacity ($>10^9$A cm^{-2}), high conductivity ($\sim10^5$S/m) and high EMI shielding effect, CNTs grab extensive attention among researchers since its discovery. Laser ablation, arc discharge and chemical vapor deposition (CVD) are well-established techniques to synthesize powdered CNTs[4, 5], but CVD is the most common technique. But in powder form, it is difficult to take advantage of electrical properties of CNTs to make them usable in numerous applications such as transistors[6], interconnectors, sensors[7], flat panel displays. For having its advantage on industrial level, macrostructure of CNTs such as CNT fiber, CNT ribbon, CNT sheet form should be assembled[8, 9]. By aligning large number of CNTs, connected *via* weak van der Waals attraction, CNT fiber can be synthesized. These can be further used for power

*Corresponding authors
(E-mail: bps@nplindia.org, dhakate@nplindia.org)

saving cables as the advancements in our technologies which raised the requirement of smart, lightweight and conducting wires for various application such as macro-computers, fuel-efficient aero vehicles, satellites etc. Moreover, these conducting fibers can be used as wiring in telecommunication industry[10] such as dipole antenna[11], USB cables[12], coaxial cables[13], transformers[14], generators, ethernet cable[15], aerospace vehicles (fighter planes), satellites and high-profile machineries[16]etc., due to less density and high flexibility than traditional Litz wires. The CNT based macro assemblies can be used as outer (CNT ribbons or CNT sheets) or inner conductor (CNT fiber) as per one's requirement. If CNTs are used as inner as well as outer conductor, the density will decrease up to 69% than regular cables[16]. CNT fibers are the best alternative for data communication applications as these fibers have negligible skin effect and proximity effect observed at high frequencies[17] which are the major reason of losses through wires. As the CNTs are aligned in bundles, the electrons transportation in CNT fiber follows variable Range hoping model[18] and tunnelling at junctions.

As per industries requirement, electric cables should be the balance of high conductivity, less density and low cost. However, the conductivity of CNT fiber is less than Cu and Al wires but due to very less density in comparison with metal conductors, CNT fibers are of great interest. Wet spinning, forest spinning and direct spinning are the reported techniques for synthesis of CNT macrostructures. Published studies revealed that pristine CNT fiber synthesized *via* direct spinning is the most preferable technique as it is a one-step process[19]. Nevertheless, the as-produced continuous fibers have good electrical conductivity and very compatible to produce hybrid fiber.

In the present work, the different growth parameters are optimized for the synthesis of CNT fibers through direct spinning of as-synthesised CNT aerogel. After optimizing, different processing parameters like temperature, pressure and argon to hydrogen ratio, CNT fibers were synthesized and then twisted. The morphology of as-twisted CNT fiber is observed *via* microscopy (optical, SEM, TEM). The room temperature electrical conductivity and R-T characteristics of as-spun CNT fibers have been studied.

2 Experimental

2.1 Materials

Ferrocene and thiophene were purchased from Hi Media Leading Bio Sciences Company. Ethanol (99.9% pure) was purchased from BRG Bio medicals, India. Above-mentioned chemicals were used in the condition they were received, without any pre chemical treatment. Argon (99.999%) and hydrogen (99.999%) were used as carrier gasses during synthesis process.

2.2 Synthesis of carbon nanotube fibers (CNT fibers)

The CNT fibers were spun from CNT sock produced in horizontal system by floating catalyst chemical vapor deposition technique. It consists a precursor purging and gas insertion chamber having syringe pump and mass flow controllers (MFCs) for Ar and H_2, synthesis chamber having split tube electric furnace with alumina reactor(inner diameter ~100mm), aerogel collecting and spinning chamber following with a vacuum circuitry (Fig. 1a). The solution of ethanol, ferrocene, and thiophene were injected in reactor with different relative contents (40 ml:0.9 gm:0.05 gm) respectively, through syringe pump at 12ml/hr. Under hydrogen atmosphere, the nanotubes formed as CNT organogel and stretched out in cylindrical hollow sock form due to the gas flow. For spinning of CNT fiber, CNT sock was pulled out from the furnace continuously and wound on a roller. The as-collected fibers (S1,S2,S3,S4) were further characterized.

2.3 Characterization

The diameters of several as-synthesized CNT fibers were measured by an optical microscope (Carl ZESSIS MA10). Raman spectroscopy (Renishaw in *Via* Reflux Raman spectrometer, 514 nm wavelength) was used to characterize the CNT fibers for the detection of defect band (D) and the band of vibrations of graphitic structures (G) in order to measure the quality of the sample. Scanning Electron Microscopy (model no. VP-EVO, MA-10, Carl-Zeiss,

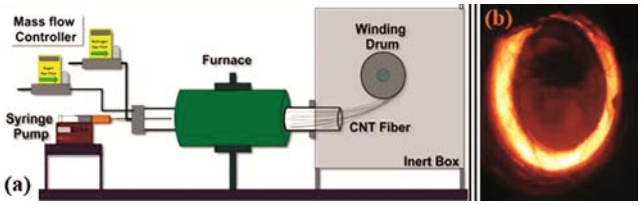

Fig. 1 — (a) Schematic of direct spinning techniue and (b) synthesized CNT aerogel.

UK, 10KV) was used to observe the material microstructure and detect the presence of carbonaceous impurities. High-resolution Transmission Electron Microscopy (model no. FEI, Tecnai T30, 300KV) was used to observe the type and diameter of CNTs contained in the fiber. It also probed for the presence of impurities. The electrical resistance measurements were performed using a two-probe method. The contacts were made with gold on Si/SiO_2 substrate *via* DC sputtering. For measurement of resistance as a function of T, CNT fiber is placed on glass substrate and contacts were made *via* using silver paint. In order to measure resistance versus temperature characteristics (R v/s T) the sample was immersed in a continuous flow helium cryostat. The R(T) characteristics were recorded on cooling from 310 K to 77 K and on heating from 77 K to 310 K. The plotted curve retraces itself in heating cycle.

3 Results and Discussion

3.1 Morphology

The morphology of CNT fiber was observed *via* optical and electron microscopies. Fibers of various diameters were synthesized *via* twisting. The minimum diameter of CNT fiber (S1) is 9.45µm. The twisting can be observed in optical image (Fig. 2a). The as-twisted fiber show high porosity. The highly packed with less porosity fibers (S2, S3) are also synthesized having large diameter (shown in fig. 2b and 2c). But all samples contain small diameters CNTs, as shown in TEM images of as synthesized fibers. Though several samples were prepared, one of them studied having ~ 43.1 µm diameter (S4). The length of fiber is 24 cm. Lengthy CNTs (shown by dotted lines) is observed in SEM image (Fig. 2h). For TEM images, CNT assemblies were dispersed in DMF for 4 hrs and then sample is taken on Cu grid.

3.2 Raman spectroscopy

Raman spectroscopy is a very powerful tool for quick confirmation of presence of CNTs[20]. Here, the Raman spectra were taken with 2.8eV laser excitation energy. Figure 3a shows the spectra, taken at four different positions (P_1, P_2, P_3 & P_4) of the sample having 43.1 µm diameter. The spectra have been fitted with Lorentzian and BWF line shapes[21]. The I_D/I_G ratio was 0.53, 0.44, 0.43, 0.49 illustrated at P_1, P_2, P_3 & P_4 respectively, showing that CNT fibers possessed low density of sp^3 carbon defects in nanotube walls. The splitting of G band as G^+ and G^-, is observable[22] and exhibits asymmetric characteristic Berit–Wigner–Fano (BWF) line shape.

Moreover, radial breathing mode (RBM) was observed in all positions which indicates the presence of less wall CNTs[23](also confirmed *via* TEM images (Fig. 2)). The RBM peaks are shown indivisually in Fig. 3b.

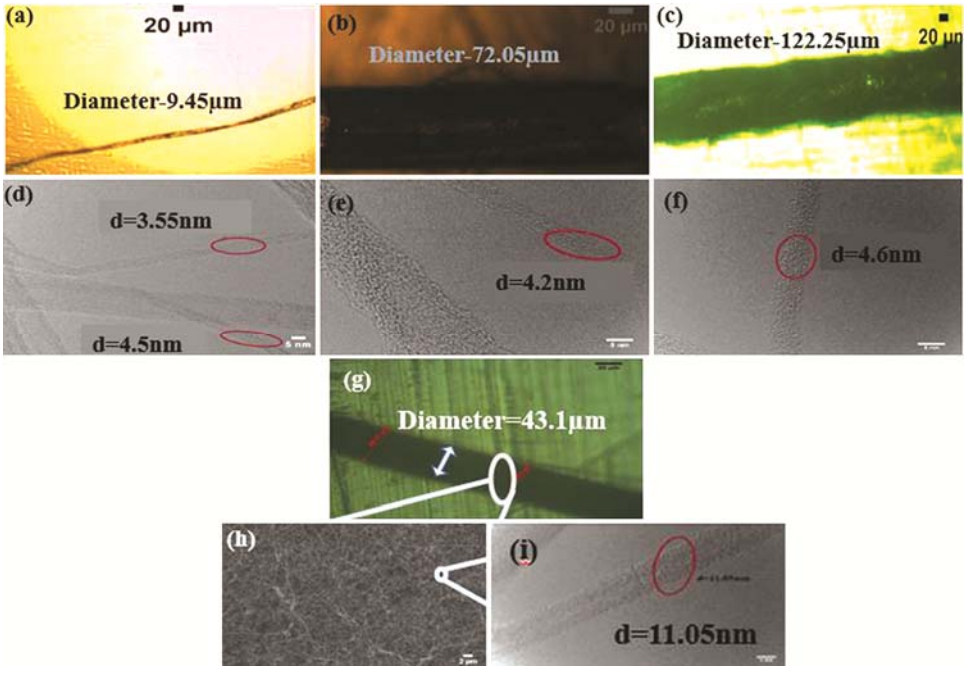

Fig. 2 — (a) Optical image of twisted CNT fiber having high porosity, (b & c) optical images of CNT fibers with less porosity, (d, e & f) TEM images of CNT fibers S1,S2, S3, (g) optical image of CNT fiber (S4), (h) SEM image S4 and (i) TEM imageof S4.

Above-mentoned asymmetric BWF line shape,described by:

$$I=\frac{Io(1+\frac{\omega-\omega o}{\Gamma})^2}{1+(\frac{\omega-\omega o}{\Gamma})^2} \quad \ldots(1)$$

The asymmetric BWF line shape of the G band also reflects the predominance of metallic SWNTs. It presents the typical broadening of metallic CNTs due to G peak arising from the tangential shear mode of carbon atoms that corresponds to the stretching mode in graphite.

According to literature, for high conductivity of CNTs, 1/q should be in range from -0.1 to -0.4 for metallic CNTs[21]. The curve fitting was done by BWF line shape and the evaluated value of asymmetric factor is -0.17 which confirms the metallicity of CNT fiber.

The presence of RBM peak in the Raman spectra, shows the presence of less wall CNTs in CNT fiber. The interpretation of the Raman spectra can be confidently applied to four different locations of CNT fiber having 43.1µm.

3.3 Energy dispersive X-Ray spectroscopy (EDS)

EDS is a quick elemental analysis technique by which qualitative composition is analysed. The EDS results of sample having 43.1µm diameter is shown in Fig. 4, reveals that particles contain predominantly carbon, as well as oxygen and iron. The wt % of iron is less which confirms the high purity of sample.

3.4 DC conductivity

Figure 5a shows the sample preparation process for conductivity measurement. As shown, gold masking is done by DC sputtering and the conducting path was 300 µm in width. After this, conductivity is measured *via* probe station used for low signal electrical characterization. In order to explore the conductive nature of as-made fibers, current v/s voltage curve was evaluated. The current is measured over a potential range of -3.5 to 3.5 V in dark and under room light at room temperature.

As per the obtained curve, the current increases linearly with respect to voltage (Fig. 5b) and

Table 1 — Curve fitting of G-peak with BWF line shape.

Γ	1/q	I_D/I_G
10.58	-0.17	0.44

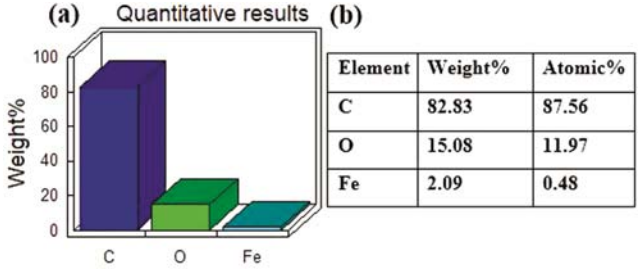

Element	Weight%	Atomic%
C	82.83	87.56
O	15.08	11.97
Fe	2.09	0.48

Fig. 4 — (a) EDS result of CNT fiber and (b) EDS table.

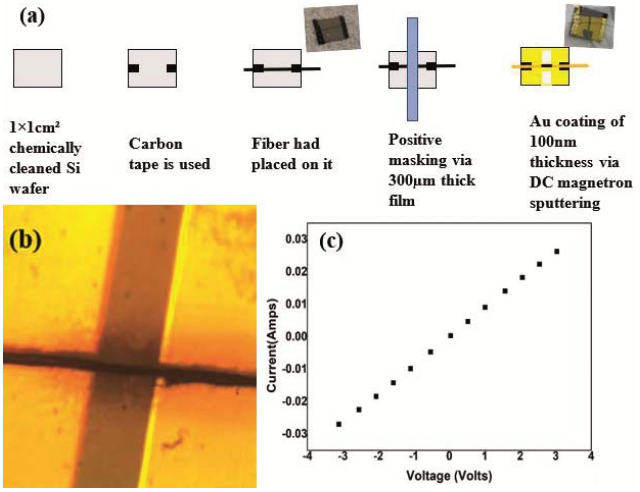

Fig. 5 — (a) Sample preparation process for conductivity measurment, (b) Optical image of gold-coated sample *via* DC sputtering and (c) I-V curve.

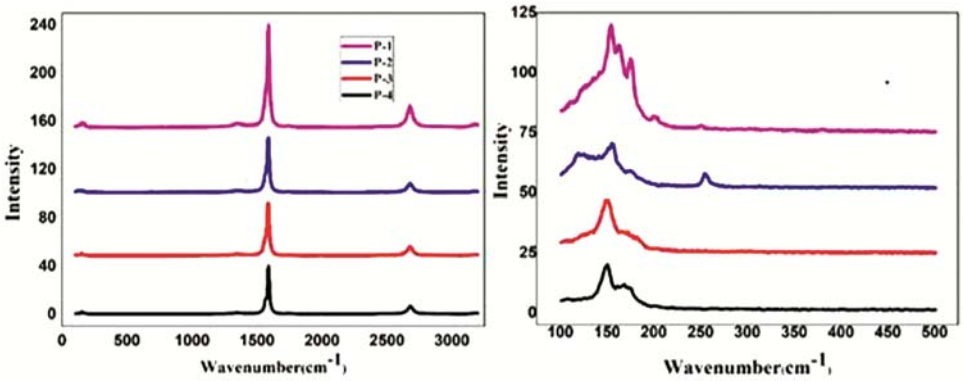

Fig. 3 — (a) Raman spectra of CNT fiber and (b) zoom spectra of RBM peak.

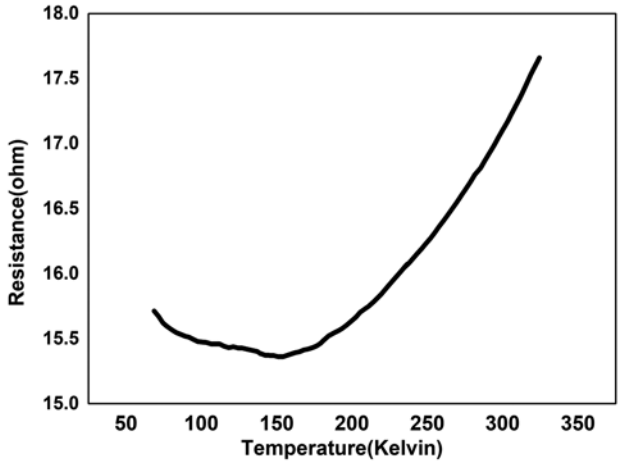

Fig. 6 — Change in resistance versus temperature plot.

follows ohmic law[24]. The measured voltage and applied current ratio was used to evaluate resistance which further used for calculation of electrical conductivity by following equation.

$$R = p\frac{l}{A} \quad \ldots(2)$$

where, p is resistivity of sample and l (300 μm) and A are the length and cross-sectional area (πr^2 where r (~74μm) measured *via* optical microscopy) of sample respectively.

By calculating resistivity, conductivity was measured *via* its reciprocal value and the evaluated electrical conductivity was 3.9×10^3 S/m. Till now, the reported conductivity of undoped CNT fiber was 10^2-10^5 S/m. Moreover, by studying the I-V curve under room light and in dark, it is concluded that there was no effect of light on conducting properties.

3.5 Resistacnce versus temperature

The change in resistance is measured with respect to temperature where helium was used to control the temperature. Vacuum pressure (10^{-2} mbar) was maintained in sampling chamber during measurement where four probe technique was used for resistance measurement. As it is reported that one-third of CNTs are metallic and others are semiconducting. These metallic CNT in CNT fiber are playing role up to 151 K (critical temperature).

Figure 6, shows the resistance versus temperature graph from 77 to 310 K of CNT fiber. There is critical temperature (T_c) below which resistance increase with decrease in temperature (similar to semiconductors). Above T_c, the curve was quite similar to metals showing PTC. Beyond that, an exponential decay of resistance with decrease in temperature can be seen up to 151 K. The temperature coefficient was measured *via* formula shown below:

$$R=R_o[1+\alpha(T-To)] \quad \ldots(3)$$

where, To is room temperature (300K).

The calculated temperature coefficient (α) is 8×10^{-4}, 5×10^{-3}, 3×10^{-3}, 2×10^{-3} at -50 °C, -100 °C, -150 °C and -196 °C respectively.

Though the change in resistance with temperature is very less which represents the less metallicity of fibers. As the critical temperature is quiet high which claims the presence of MWCNTs having different chirality.

The curve above 151 K is fitted with polynomial P(T) as shown below :

$$P(T) = 1+\beta T+\gamma T^2 \quad \ldots(4)$$

After curve fitting, numeric value of β and γ are -8×10^{-4} and 3.4×10^{-6} which is equivalent to metallic CNT fibers[25].

4 Conclusions

In this study, CNT fiber spun from CNT aerogel *via* direct high temperature CVD synthesis showed the presence of predominance of metallic CNTs. The metallic character was manifested by the broadening of the Raman G band, with a Breit-Wigner-Fanoline shape with an asymmetric factor q ranging from -0.14 to -0.4, in agreement with metallic CNTs values. The conductivity of as-made fiber was quite high (3.9×10^3S/m) because the lengthy CNTs are present in CNT fibers. The other reason of high conductivity is its purity, which is also justified *via* G-peak of Raman spectrum. Furthermore, the metallic behaviour is also confirmed *via* R-T curve as CNT fiber shows positive temperature coefficient. These high conducting CNT fibers have excellent electrical properties which can be used in wide-range electric applications.

Acknowledgement

I would like to express my gratitude to Dr Sudhir Husale and Dr. H.K. Singh for DC conductivity measurement and R-T characteristics measurement, respectively. Mrs. Shaveta Sharma is also thankful for Raman spectroscopy measurements.

References

1 Behabtu N, Young C C, Tsentalovich D E, Kleinerman O, Wang X, Ma A W, Bengio E A, ter Waarbeek R F, de Jong J J & Hoogerwerf R E, *Sci,* 339 (2013) 182.

2 Janas D, Vilatela A C & Koziol K K, *Carbon,* 62 (2013) 438.

3 Iijima S, *Nature,* 354 (1991) 56.

4 Öncel Ç & Yürüm, Y, Fullerenes, Nanotubes, and Carbon Nonstructures, (Taylor & Francis, UK) 14 (2006) 17.

5 Mathur R B, Singh B P & Pande S, Carbon Nanomaterials: Synthesis, Structure, Properties and Applications (Taylor & Francis, UK), 1st Edn, ISBN: 9781498702102 (2016) 284.

6 Steiner M, Engel M, Lin, YM, Wu Y, Jenkins K, Farmer D B, Humes J J, YoderN L, Seo JW T & Green A A, *Appl Phys Lett,* 101 (2012) 053123.

7 Bastatas L D, Echeverria-Mora E, Wagle P, Mainali P, Austin A & McIlroy D N, *ACS Sens,* 3 (2018) 2367.

8 Janas D & Koziol KK, *Nanoscale,* 8 (2016) 19475.

9 Sharma S, Arya A K, Dhakate SR, Singh BP, Organized Networks of Carbon Nanotubes, (Taylor & Francis,UK), 1st Edn, ISBN: 9780367278205 (2020) 75.

10 Amram Bengio E, Senic D, Taylor L W, Headrick R J, King M, Chen P, Little C A, LadburyJ, Long C J & Holloway C L, *Appl Phys Lett,* 114 (2019) 203102.

11 Amram Bengio E, Senic D, Taylor L W Tsentalovich D E, Chen P, Hollowa, C L, Babakhani A, Long C J, Novotny D R & Booth J C, *Appl Phys Lett,* 111 (2017) 163109.

12 Guo H, Dewey O, McCorkle L S, Meador M A B & Pasquali M, *ACS Appl Polym Mater,* 1 (2019) 1680.

13 Jarosz P R, Shaukat A, Schauerman C M, Cress C D, Kladitis P E, Ridgley R D & Landi B J, *ACS Appl Mater Interfaces,* 4 (2012) 1103.

14 Kurzepa L, Lekawa-Raus A, Patmore J & Koziol K, *Adv Funct Mater,* 24 (2014) 619.

15 Jarosz P, Schauerman C, Alvarenga J, Moses B, Mastrangelo T, Raffaelle R, Ridgley R & Landi B, *Nanoscale,* 3 (2011) 4542.

16 Alvarenga J, Jarosz P R, Schauerman C M, Moses B T, Landi B J, Cress C D & Raffaelle RP, *Appl Phys Lett,* 97 (2010) 182016(1)- 182016(3).

17 Lekawa-Raus A, GizewskiT, Patmore J, Kurzepa L & Koziol K K, *Scr Mater,* 131 (2017) 112.

18 Fogler M, Teber S & Shklovskii B, *Phys Rev B,* 69 (2004) 035413.

19 Li YL, Kinloch I A & Windle A H, *Science* 304 (2004) 276.

20 Gupta R, Singh B P, Singh VN, Gupta T K & Mathur RB, *Carbon,* 66 (2014) 724.

21 Brown S, Jorio A, Corio A P, Dresselhaus M, Dresselhaus G, Saito R & Kneipp K, *Phys Rev B,* 63 (2001) 155414.

22 Costa S, Borowiak-Palen E, Kruszynska M, Bachmatiuk A & Kalenczuk R, *Mater Science-Poland,* 26 (2008) 433.

23 Zhang Y, Zhang J, Son H, Kong J & Liu Z, *J Am Chem Soc,* 127 (2005) 17156.

24 Mikhalchan A, Fan Z, Tran T Q, Liu P, Tan V B, Tay T E & Duong H M, *Carbon,* 102 (2016) 409.

25 Dini Y, Faure-Vincent J & Dijon J, *Nano Res,* 13 (2020) 1764.